Determination of Orientation in Thermotropic Liquid Crystalline Polymer Films by Spectrographic Measurement of the Birefringence

F. Beekmans‡ and A. Posthuma de Boer*

Delft University of Technology, Faculty of Chemical Technology and Materials Science, Department of Polymer Technology, Julianalaan 136, 2628 BL Delft, The Netherlands

Received June 14, 1996; Revised Manuscript Received September 17, 1996⊗

ABSTRACT: The degree of orientation in thermotropic liquid crystalline polymer films has been determined as a function of the draw ratio using a specially developed spectrographic birefringence technique, diffuse reflectance infrared spectroscopy (DRIFT), and wide-angle X-ray scattering (WAXS). Quantitative measurements of the average birefringence were obtained despite the huge turbidity of the samples. The order parameter calculated from the birefringence was found to depend on the draw ratio according to the Kuhn and Grün equation for pseudo-affine deformation. The infrared dichroism was measured as a function of film thickness by layer removal. The thickness-averaged orientation calculated from the DRIFT measurements also indicated affine deformation of the films. The orientation derived from WAXS appeared to be clearly overaffine. The difference between the results from WAXS and the results from the other two techniques is attributed to preferential orientation of the crystalline fraction due to flow-induced crystallization in the films which is detected only by WAXS.

Introduction

Liquid crystalline polymers (LCPs) owe their name to the duality of their liquid state. They show liquidlike behavior in the solution or in the melt, retaining, however, a high degree of local molecular orientation reminiscent of the solid state. The local molecular ordering is the consequence of the chemical structure of these polymers, having rigid anisometric parts in their main chain or side chains. A general feature of the liquid crystalline state of polymers is the relative ease of obtaining flow-induced orientation on a mesoscopic or macroscopic scale. This enables manufacturing products with unique properties because of the high degree of anisotropy. The relative ease of introducing orientation is especially exploited in main-chain LCPs, which are mainly used in mechanical or structural applications. Well-known examples are aramids, from which high modulus fibers are obtained by spinning from a liquid crystalline solution, and aromatic ester/ester or ester/amide copolymers, which can be melt-processed due to their thermotropic nature.

Knowledge of the degree of orientation of LCPs, on the molecular, mesoscopic, and macroscopic scales, is crucial to understanding the behavior of LCPs and to correlating properties and processing conditions. This holds especially for thermotropic liquid crystalline polymers, which are usually subjected to complex flows during processing by extrusion or injection molding. The degree of orientation in the final product is highly dependent on a combination of the flow type (elongation or shear), the flow rate, the duration of flow and relaxation effects. More than with flexible polymers, the processing conditions determine the microstructure and, therefore, the properties of the final product.

Many reports are concerned with the characterization of the molecular orientation in final products of thermotropic LCPs, like injection molded parts. Techniques commonly used are polarized optical microscopy, X-ray scattering, and (reflection or photoacoustic) infrared dichroism.[1−11] Often a layered structure is found parallel to the flow direction, in which the orientation differs from one layer to another. The processing conditions highly influence the number of layers, the thickness of the layers, and the orientation inside the layers, which in turn influence the (ansiotropy of the) mechanical properties, the coefficient of expansion, and the form stability.[12] Far fewer reports have appeared concerning the structure evolution during flow of thermotropic LCPs, describing mainly qualitative measurements.[13−19] Yet, detailed understanding of the interrelation between rheological behavior and structure development in the liquid crystalline state is crucial, just as for lyotropic LCPs, for which a substantial number of both qualitative and quantitative rheo-optical investigations have been reported.[20−28]

Techniques that are in principle suitable for assessing changes in polymer structures are X-ray diffraction and optical analysis including birefringence and light scattering. A requirement for such measurements is that the flow cell used is transparent to the waves applied. High intensities and sensitive detectors are required for sufficient time resolution of the measurements. For X-ray measurements this results in the necessity of using synchrotron radiation.[17,25] For optical studies an additional problem is the high level of light scattering caused by the fine polydomain texture, which makes small gap sizes (≤ 25 μm) in the flow cell necessary. Further, for thermotropic LCPs a flow cell is required that is able to operate at temperatures of approximately 300 °C. Therefore, rheo-optical studies of thermotropic LCPs have not received much attention, in contrast to lyotropic LCPs.

In this paper we describe a spectrographic birefringence technique for the determination of orientation in thermotropic LCPs. This technique has been designed for rheo-optical experiments on highly birefringent materials. It is based on the same principles as techniques used for lyotropic LCPs under shear flow.[21,22,28] Results are reported for drawn solid films of the thermotropic LCP Ultrax KR4002. The aim of

* To whom correspondence should be addressed.
‡ Current address: ATO-DLO, Bornsesteeg 59, P.O.Box 17, 6700 AA Wageningen, The Netherlands.
⊗ Abstract published in *Advance ACS Abstracts,* December 1, 1996.

S0024-9297(96)00860-1 CCC: $12.00

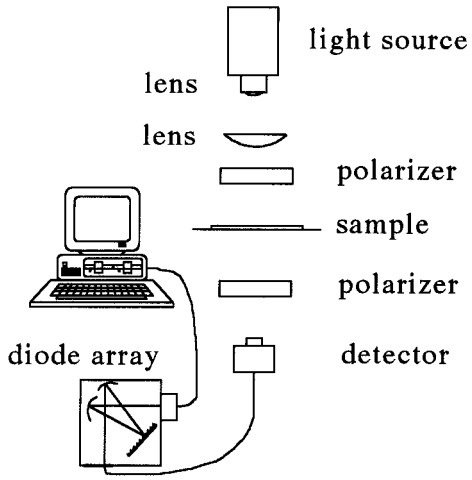

Figure 1. Schematic illustration of the optical setup for spectrographic birefringence measurements.

this research is to demonstrate the feasibility of this method for measurement of orientation of highly scattering thermotropic LCPs, and to optimize the technique for future quantitative rheo-optical experiments. Therefore, the results are compared to data obtained by techniques well-established for solid samples, i.e. infrared dichroism and wide-angle X-ray scattering (WAXS).

Experimental Section

Sample Preparation. The liquid crystalline polymer investigated in this work was the commercially available thermotropic LCP Ultrax KR4002 from BASF. Its main constituents, according to the supplier, were 1,4-hydroxybenzoic acid, terephthalic acid, and 2,7-dihydroxynaphthalene, unfortunately, in an unknown composition. The LCP was thermally characterized with DSC measurements (Perkin-Elmer, DSC-7). It exhibited a glass transition temperature of 128 °C and a crystal−nematic transition in the range of 272−298 °C, which was sometimes difficult to detect. Annealing of the polymer for 1 h at 270 °C resulted in a melting point of about 310 °C. A similar annealing effect has been reported in the literature for HBA/HNA random copolyesters.[30] The as-received pellets were dried at 150 °C for 4 h in a nitrogen atmosphere and stored in a vacuum oven at 60−80 °C. The thermotropic LCP was extruded in a Collin single screw extruder equipped with a slit die. Three slit heights, 0.2, 0.5, and 1mm, were used to obtain sufficiently thin samples to be able to do the birefringence measurements over a wide range of draw ratios. The width of the die was 100 mm, and the temperature of the extruder and the die were 300 and 280 °C, respectively. After leaving the die, the polymer film was stretched by a winding mechanism and quenched by an air flow within 100 mm from the die exit. Draw ratios between 1.5 and 65 could be obtained by changing the takeup speed, where the draw ratio was calculated as the quotient of the surface of the cross-section at the die outlet and of the solid film. The orientation measurements were all performed at ambient temperatures.

Spectrographic Birefringence Technique. The spectrographic birefringence technique was first introduced and treated in much detail by Hongladarom et al.[21,22] In Figure 1 a schematic illustration of our setup is shown. The optical train starts at a 400 W xenon white light source (Oriel) that provides an intensity high enough to obtain a sufficient signal at the detector over a wide wavelength range despite the extreme turbidity of the samples. Using a lens and collimation system a parallel beam is created with a spot size of about 4 mm. The polymer film is placed perpendicular to the propagation direction of the light beam between two parallel or crossed polarizers, the directions of polarization of which are set at ±45° with reference to the stretch direction of the sample. Both spectra for parallel and crossed polarizers were recorded. The detector system consists of a quartz optical fiber that leads to a grating spectrograph (Oriel Multispec), which in turn splits the beam and projects the spectrum (300−800 nm) onto a diode array (1024 pixels) with a resolution of 1.8 nm. The collection of one spectrum requires 40 or 80 ms depending on the turbidity of the sample, and for one measurement the data are averaged 16 times.

Mueller matrix analysis of the optical train, neglecting any dichroism, yields the following equations for the light intensity transmitted through a pair of crossed (⊥) or parallel (||) polarizers and the sample:

$$I^{\perp} = \frac{I_0}{2} e^{-2\alpha} \sin^2\left(\frac{\pi \Delta n d}{\lambda}\right) \tag{1}$$

$$I^{\parallel} = \frac{I_0}{2} e^{-2\alpha} \left[1 - \sin^2\left(\frac{\pi \Delta n d}{\lambda}\right)\right] \tag{2}$$

In these equations I_0 is the intensity of the incident beam with wavelength λ, Δn is the birefringence, d is the sample thickness, and $e^{-2\alpha}$ is a term that accounts for the attenuation of light due to isotropic absorption or scattering. Normalized, these equations give

$$N^{\perp} = \frac{I^{\perp}}{I^{\perp} + I^{\parallel}} = \sin^2\left(\frac{\pi \Delta n d}{\lambda}\right) \tag{3}$$

$$N^{\parallel} = \frac{I^{\parallel}}{I^{\perp} + I^{\parallel}} = \cos^2\left(\frac{\pi \Delta n d}{\lambda}\right) \tag{4}$$

and

$$N^{\parallel} - N^{\perp} = \cos\left(\frac{2\pi \Delta n d}{\lambda}\right) \tag{5}$$

Equations 3−5 are independent of I_0 and the attenuation term $e^{-2\alpha}$. Thus, fitting the normalized intensity versus wavelength curve easily leads to the birefringence.

The birefringence is for a nematic directly related to the order parameter S or $\langle P_2 \rangle$,[31] which is the degree of orientation of the molecular main chains around the director **n** and is defined by the second-order Legendre polynomial:

$$\frac{\Delta n}{\Delta n_{\max}} = S = \langle P_2 \rangle = \frac{1}{2}(3\langle \cos^2\theta \rangle - 1) = 1 - \frac{3}{2}\langle \sin^2\theta \rangle \tag{6}$$

where $\langle ... \rangle$ represents an average over the orientation distribution function and θ is the angle between an individual molecule and the director (the angular brackets around P_2 are omitted in the remaining text). $\Delta n_{\max}$ is the maximum birefringence determined by the values of the refractive indices parallel and perpendicular to the polymer chain. Equation 6 holds for a monodomain only, i.e. in case there is no additional spatial inhomogeneity. Larson and Doi[32] proposed the concept of a mesoscopic order parameter P_2^{dom} that accounts for the existence of a polydomain texture. P_2^{dom} is the degree of director orientation averaged over the domain orientation distribution function. Hence the experimentally measured order parameter is composed of contributions from the molecular level (P_2^{mol}) and from the domain level (P_2^{dom}):

$$P_2^{\mathrm{exp}} = P_2^{\mathrm{mol}} P_2^{\mathrm{dom}} \tag{7}$$

With birefringence, where the spot size of the light is usually much larger than the domain size, only this overall order parameter can be obtained. Determination of the molecular order parameter requires either a monodomain sample or a special technique like solid-state NMR.

Wide-Angle X-ray Scattering (WAXS). X-ray photographs were taken of the stretched thermotropic LCP films in our laboratory, using a Kiessig camera connected to a Philips PW 1130 generator that produces Ni-filtered Cu Kα radiation. The X-ray beam was 1 mm in diameter and the

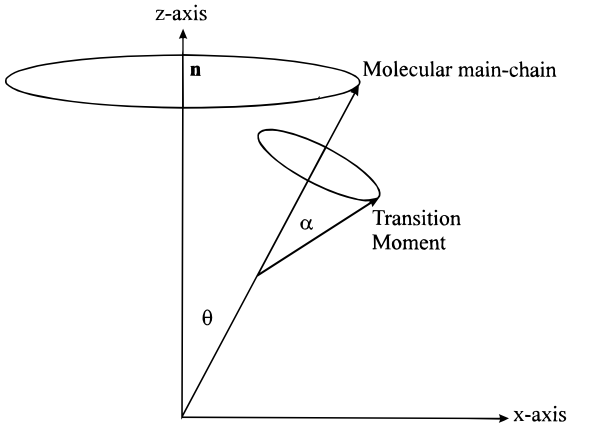

Figure 2. Coordinate system including relevant angles for infrared dichroism measurements of a monodomain sample. In the case of a polydomain sample the director **n** can also have an angle with the *z*-axis.

distance from the sample to the photographic film was mostly 100 mm and for some measurements 50 mm. The exposure times were between 16 and 24 h (for the 100 mm sample−film distance) depending on the sample thickness. A few photographs were made of a stack of drawn samples with the X-ray beam parallel to the film surface to see if there is any biaxiality in the films. The strong equatorial reflections of photographs with a sample−film distance of 100 mm were scanned at Akzo-Nobel research laboratories with a Joyce Loebl Microdensitometer Mk III cs, that was able to perform the azimuthal scan. From the digitized data the order parameter was determined by averaging the $\sin^2 \alpha$ over the distribution function, where α is the angle between the equator and the normal to a crystal plane. The distribution function was either the intensity curve of the raw data or a fit with a Pearson VII function.[33] Because an averaging of the equatorial reflection was used instead of the meridional reflection, the so obtained $\langle \sin^2 \alpha \rangle$ had to be multiplied by 2 in order to get $\langle \sin^2 \theta \rangle$, the average required for determination of the order parameter with eq 6.[34−36]

Infrared Dichroism. Diffuse reflectance infrared spectroscopy (DRIFT) was used to determine the orientation, since even for the thin films (20 μm) the absorption of infrared light in transmission experiments was too high. The spectra were collected with a Mattson Polaris high-resolution FTIR spectrometer equipped with a wire grid polarizer (1200 aluminum l/mm on a zinc selenide substrate, range 500−5000 cm^{-1}, Specac) and a DTGS detector. The resolution was 8 cm^{-1}, and the spot size was comparable to the birefringence measurements, i.e. 4−5 mm. The influence of the absorption on the amplitudes of the spectral features of the specular reflectance scan was eliminated by using light polarized perpendicularly to the plane of reflection (s-polarization).[37] Reflectances parallel and perpendicular to the draw direction was measured twice by turning the sample fully around on a flat turntable. Results of opposite measurements were averaged to eliminate nonplanarity of the sample. The specular reflectance spectra were differentiated to obtain spectra suitable for interpretation.[9,38] No difference was found between simple differentiation and the more correct Kramers−Kronig transformation.

The dichroic ratio R is defined as

$$R = \frac{A_{\parallel}}{A_{\perp}} \tag{8}$$

$A_{\parallel}$ and $A_{\perp}$ being the absorptions parallel and perpendicular to the draw direction (*z*-direction in Figure 2). The order parameter was calculated from the dichroic ratio by[39]

$$P_2 = \frac{R-1}{R+2}\frac{R_0+2}{R_0-1} \tag{9}$$

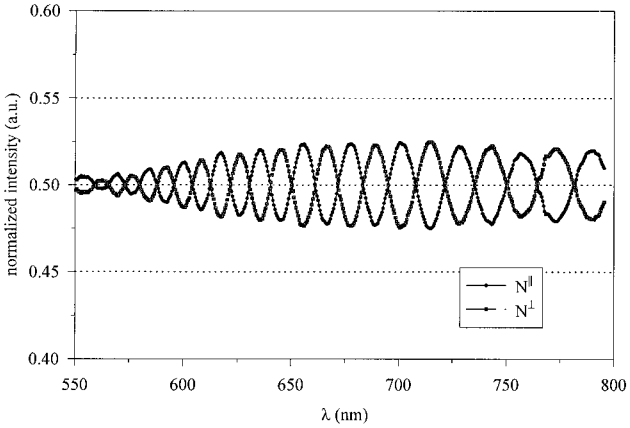

Figure 3. Normalized intensity versus wavelength using eqs 3 and 4.

where R_0 is the dichroic ratio for the case of perfect molecular alignment. R_0 is directly related to the inclination angle α of the transition moment (see Figure 2):

$$R_0 = 2 \cot^2 \alpha \tag{10}$$

For uniaxial systems assuming that the sample is transversely isotropic, eq 9 can also be expressed as

$$P_2 = \frac{P_2^{\,IR}}{P_2^{\,\alpha}} \tag{11}$$

where P_2^{IR} is the measured quantity $(R-1)/(R+2)$ in eq 9, which is the overall misalignment. P_2^{α} is the value of the second-order Legendre polynomial for angle α, which is a correction factor that is required because of the inclination of the transition moment to the molecular axis. Because the spot size of the infrared beam is much larger than the average domain size, the order parameter determined with this technique is comparable to the experimental order parameter P_2^{exp} in eq 7.

Although the effective penetration depth of the infrared light with this technique was estimated to be a few microns only, special care was taken to remove the minor reflections from the back of the sample by mounting the films on a polyethylene substrate with an immersion oil in between.[38] Due to the small penetration depth the orientation measured on the surface of the sample did not reflect the average orientation that was measured with birefringence and X-ray diffraction. Therefore, layers were removed by careful grinding to obtain a depth profile of P_2. From the depth profile an average order parameter was calculated that could be compared to the values obtained from the other techniques used.

Results

Spectrographic Birefringence. Figure 3 shows the intensity versus wavelength curves normalized according to eqs 3 and 4. They are shown in the range from 550 to 800 nm only, because below 550 nm the signal is too weak. Obviously, the amplitude of the measured oscillations is very small and not constant, and the period varies locally. This variation in amplitude and period is not systematically related to the sample thickness but is sample-dependent. The fact that an oscillation is observed at all can, however, only be attributed to the existing birefringence in the sample. The reason that the normalized intensity curves do not resemble a true $\cos^2$ or a $\sin^2$ with amplitudes between 0 and 1 originates from depolarization and polarization mixing due to the polydomain texture not accounted for in eqs 1 and 2.[21,22] A more adequate description of the transmission intensity should include an extra term

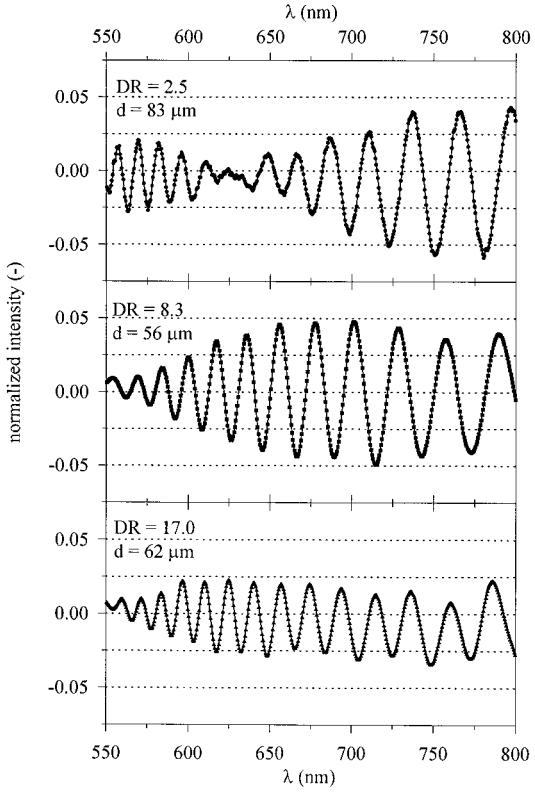

Figure 4. Normalized intensity versus wavelength for three films with different draw ratios. The curves have been obtained from the raw data by normalization with eq 5.

accounting for depolarization effects. The transmission equations (1) and (2) can be modified as follows:[16,40]

$$I^{\perp} = F \sin^2\left(\frac{\pi \Delta n d}{\lambda}\right) + T_s \qquad (12)$$

$$I^{\parallel} = F\left[1 - \sin^2\left(\frac{\pi \Delta n d}{\lambda}\right)\right] + T_s \qquad (13)$$

where F is the attenuation of light resulting from absorption, scattering, or reflection (comparable to the term $e^{-2\alpha}$ in eqs 1 and 2) and T_s is the transmittance of the sample arising from depolarization or leakage from the polarizers. Normalization of eqs 12 and 13 similar to eqs 3 and 4 results in equations with a reduced amplitude and an additional term. Both this reduced amplitude and additional term depend on the amplitude term F and the depolarization term T_s. For large depolarization this normalization results in a curve with a much reduced amplitude, superimposed on the additional term of approximately 0.5, as observed in Figure 3. When eq 5 is used to normalize the intensity equations (12) and (13) the additional term drops out and a cosine curve with a reduced amplitude is obtained, oscillating around 0. Figure 4 shows three examples for different draw ratios.

Hongladarom et al.[21] fitted their curves directly with a $\sin^2$ or $\cos^2$ function, including a wavelength dispersion function to obtain the correct fit. The present curves are not as neat as theirs and, therefore, we circumvent the difficult fitting procedure by determining the periods of oscillations from which the birefringence is calculated at various wavelengths. This is done by determining all zero crossings, λ_i, and the midpoints between these crossings, $\lambda_m = {}^1/_2(\lambda_{i+1} + \lambda_i)$. Assuming that the birefringence does not change much between two subsequent zero crossings, it can be approximated by

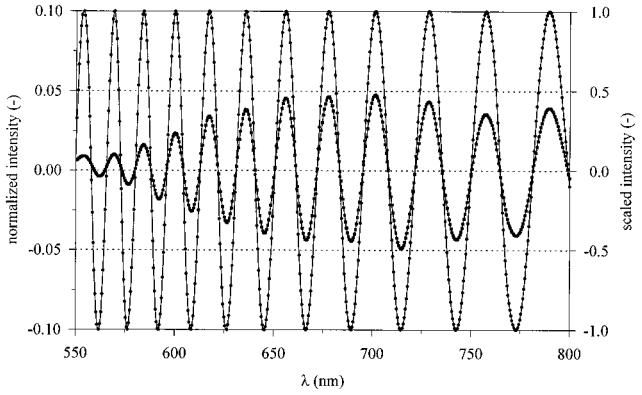

Figure 5. Scaling of the normalized intensity curve for the film with DR = 8.3 of Figure 4.

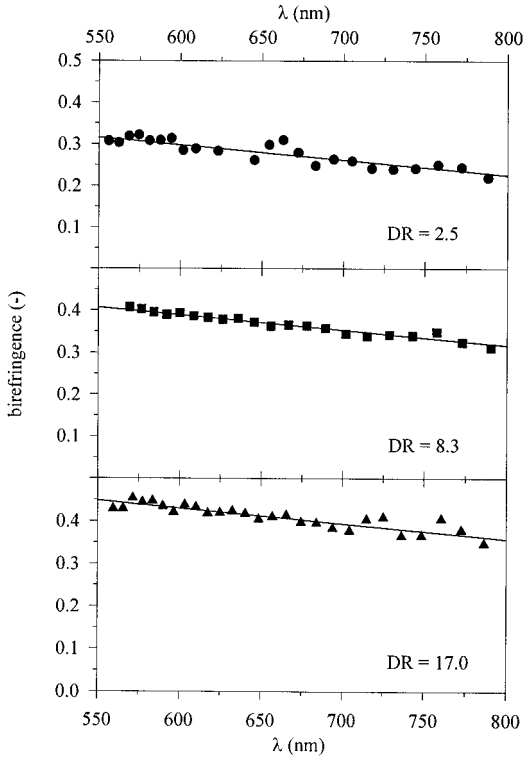

Figure 6. Birefringence versus wavelength for the three examples of Figure 4.

$$\Delta n \approx \frac{\lambda_i \lambda_{i+1}}{2d(\lambda_{i+1} - \lambda_i)} \approx \frac{\lambda_m^2}{2d(\lambda_{i+1} - \lambda_i)} \qquad (14)$$

This approach, of course, works only if the observed zero crossings are closely spaced, like in our results.

In order to determine the zero crossings in those cases where the normalized intensity curves are not symmetrical with reference to the zero value, as is the case in Figure 4 for DR = 17, the normalized curves are scaled to maximum values of ±1, from which the zero crossings can unambiguously be determined. An example of a normalized intensity curve and its associated scaled version is shown in Figure 5. All birefringence values reported in this article have been calculated from these scaled normalized intensity curves.

The birefringences calculated accordingly refer to the midpoints λ_m, which are the wavelengths used in Figure 6 for plotting Δn versus the wavelength, showing immediately the (experimentally obtained) wavelength

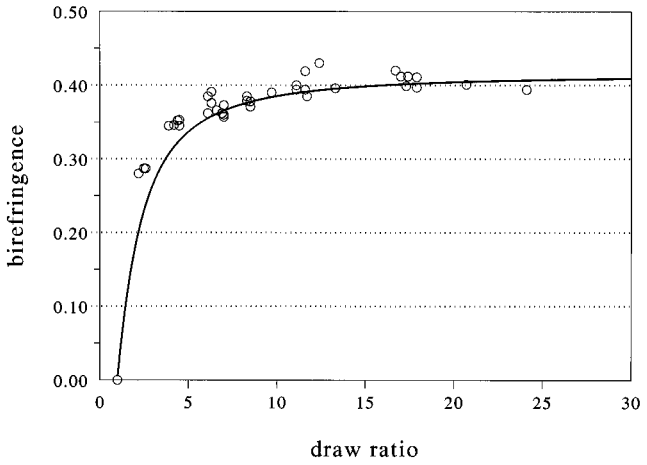

Figure 7. Birefringence versus draw ratio: (○) experimental data; (—) pseudo-affine deformation.

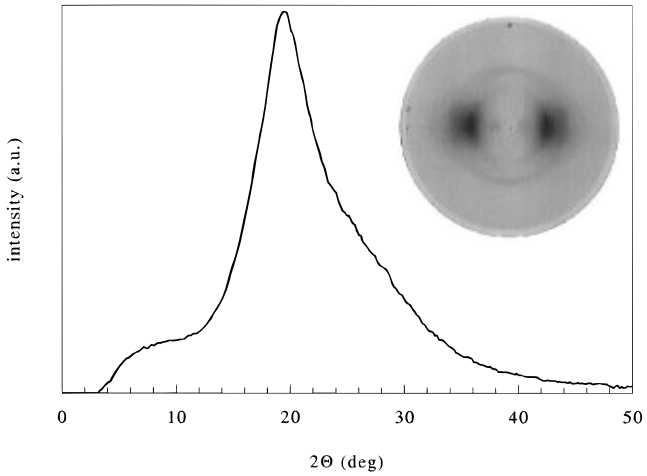

Figure 8. WAXS photograph and its radial scan in the equatorial direction. Distance sample−film = 50 mm.

dispersion for this system. Hongladarom et al. suggested a cubic relationship as a general approximation for this dispersion and calculated the coefficients for this relationship from monodomain birefringence measurements. The present results can, over the relevant part of the spectrum, well be represented by a straight line with a slightly negative slope, that turned out to be approximately equal for all experiments. One single slope was, therefore, used to fit the experimental data and the birefringence was calculated at 633 nm. In Figure 6 the three examples of Figure 4 are shown again.

Optical microscopy shows that the samples consist of an elongated polydomain texture. The width of the domains is of the order of 1 or 2 μm, and the length (which is difficult to determine) is of the order of 10 μm or more. No monodomain was observed for any draw ratio. Sampling with a beam of 4 mm diameter, therefore, leads to an average birefringence over many domains and to an overall order parameter P_2^{exp} as defined in eq 7.

The existence of an elongated domain texture suggests that the samples should exhibit a considerable dichroism due to anisotropic scattering. Dichroism values ranging from 10^{-4} to 10^{-3} have been measured, depending on the draw ratio. Neglecting the dichroism in deriving eqs 1−5, therefore, results in an error in the birefringence of about 2.5−5%. This value is within the accuracy of our experiments and of no great influence on the purpose of our work.

All birefringence data calculated for $\lambda_m = 633$ nm are plotted versus the draw ratio (DR) in Figure 7. Every point shown is a single measurement and the trend is obvious, although there is a considerable amount of experimental scatter. The scatter is most probably caused by differences in local draw ratios, because the films were not homogeneous in thickness. Duplicate measurements of the same samples at the same spot show that the individual values are correct. No birefringence has been detected for an isotropic sample. Between draw ratio values of 1 and 2.2 we have not been able to perform valid birefringence measurements because of the thickness of these samples. Figure 7, therefore, shows an empty part. The first measurable point (DR = 2.2) already has quite a high birefringence and the value starts to level off at a draw ratio between 10 and 15. The drawn curve is the Kuhn and Grün equation for pseudo-affine deformation, with a limiting birefringence value of 0.415:[41,42]

$$P_2 = \frac{1}{2}\left[\frac{3}{1-k^2} - \frac{3k\cos^{-1}k}{(1-k^2)^{3/2}} - 1\right] \qquad (15)$$

where k is $(DR)^{-3/2}$. The very high limiting birefringence value is in accordance with values reported for LCP fibers.[43] The experimental data follow the affine deformation curve quite well.

From these results a preliminary conclusion can be drawn that the spectrographic birefringence technique is able to measure orientation in solid thermotropic liquid crystalline polymers despite the huge turbidity of the samples. To test if the measured values are in the right order of magnitude, the data are now compared to infrared dichroism and WAXS results.

Wide-Angle X-ray Scattering. Figure 8 shows a WAXS photograph taken with a sample−film distance of 50 mm together with its radial scan along the equator. The photograph exhibits only a few reflections on the equator and hardly any on the meridian. The strongest peak located on the equator is caused by planes with a d spacing of 4.54 Å. From the radial scan (more clearly visible for a sample−film distance of 100 mm) a shoulder can be observed at slightly higher angles originating from a second peak hidden underneath the large peak. This peak is caused by planes with a d spacing of 4.29 Å and might indicate an orthorhombic unit cell with almost equal a and b distances.[44] No significant difference is found between azimuthal scans of both peaks. Hence, the larger peak (at 4.54 Å) is used to obtain the order parameter. The same peak also has been used by Hsiung and Cakmak[7] to investigate the structural layering phenomena in injection molded Ultrax samples by using a microbeam X-ray diffraction technique. This peak, however, consists of contributions from the crystalline phase but also from the quenched nematic phase, since the "amorphous" scattering is spread over an area containing this crystalline peak. Nevertheless, the azimuthal scans can accurately be described by a Pearson VII function (see Figure 9): correlation coefficients of 0.98−0.99 are obtained. No attempt is, therefore, made to improve this fit by using two distribution functions, a sharp one for the crystalline and a broad one for the "amorphous" part, as reported for semicrystalline polymers.[45] Hence, the order parameter deduced from WAXS, reported in this article, is mainly determined by the crystalline phase, but partly reflects the order of the quenched nematic phase as well.

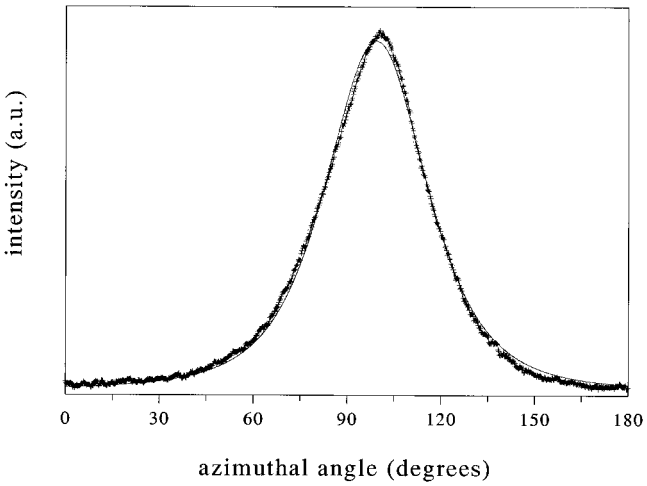

Figure 9. Azimuthal scan of the equatorial reflection at 4.54 Å with the Pearson VII fit for a film with DR = 2.5: (+) raw intensity scan; (—) Pearson VII fit.

Table 1. Order Parameter from WAXS

draw ratio	P_2 (raw curve)	P_2 (P-VII fit)
2.2	0.71	0.70
2.6	0.77	0.75
4.5	0.79	0.77
6.1	0.8	0.78
12	0.81	0.78
17	0.82	0.79
24	0.82	0.79

In Table 1 the order parameter determined from the raw intensity curves itself and from the Pearson VII fit are shown for various draw ratios. There is only a small difference between the two methods. In further comparison with other techniques the results obtained from the Pearson VII fits will be used, because the raw curves sometimes show problems with the baseline resulting in an erroneous order parameter. No significant difference could be observed between the azimuthal densitometer scans of WAXS photographs perpendicular and parallel (of a stack of drawn samples) to the surface of the samples and, therefore, the films are believed to be transversely isotropic.

Assuming that at high draw ratios the order parameter for birefringence and WAXS become equal, a scaled order parameter from the birefringence data can be deduced using the highest value for the order parameter from WAXS (P_2 = 0.79). Using eq 6 the maximum birefringence is calculated to be $\Delta n_{max} = 0.50$. This in turn is used to calculate an order parameter for the other birefringence data. The results from both techniques are shown in Figure 10. The drawn curve is again the pseudo-affine deformation (eq 15) with a limiting value of P_2 of 0.83. It is clearly seen that at low draw ratios the order parameters from WAXS are much higher than the birefringence results, while at high draw ratios the values (of course) become similar.

Infrared Dichroism. Figure 11 shows examples of the differentiated infrared spectra of the absorption parallel and perpendicular to the film stretch direction. It is clearly seen that there is a considerable amount of dichroism, i.e. several absorption bands show orientation dependent intensities. Although the dichroic ratio can be determined for many bands, the one at 1745 cm^{-1} proved to be most reliable for the determination of the order parameter with eq 9. This band can be interpreted as the transition moment of the C=O stretching, which absorbs more in the perpendicular direction than

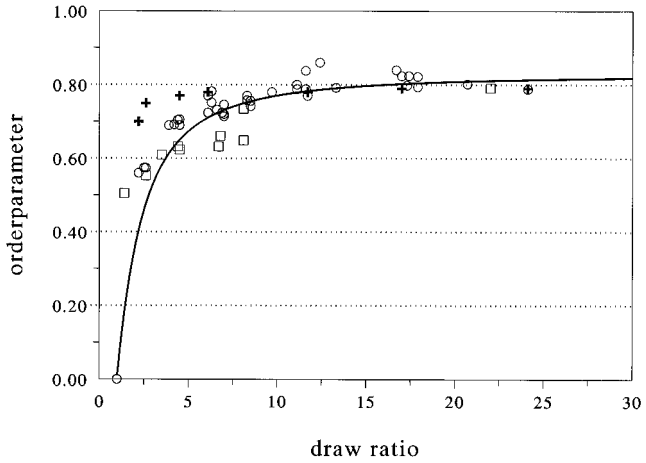

Figure 10. Order parameter from birefringence (○), WAXS (+), and infrared dichroism (□) versus draw ratio: (—) pseudo-affine deformation.

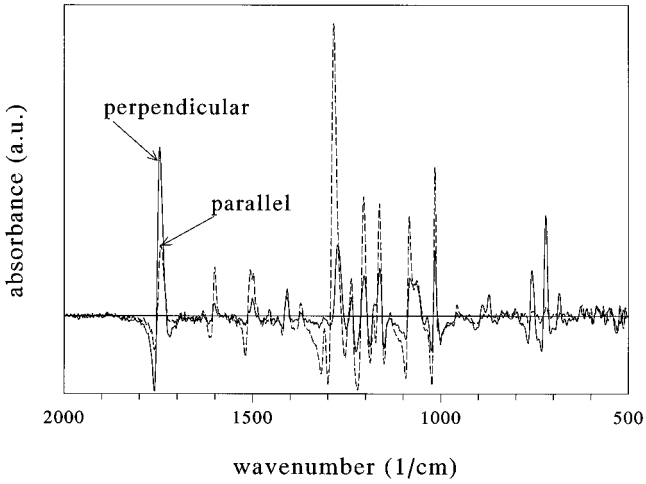

Figure 11. Differentiated infrared reflectance spectra for a film parallel and perpendicular to the infrared polarization.

in the parallel direction. Unfortunately, the angle of the carbonyl group with the main chain is unknown. Hence, the absolute value for the order parameter cannot be determined directly. Only the trend of the changing uncorrected order parameter with increasing draw ratio is obtained. However, if one again assumes that at high draw ratios the order parameter for infrared dichroism is comparable to the order parameter obtained from WAXS, an angle α can be calculated from the maximum values of both techniques. With a maximum P_2 of 0.79 for WAXS and a maximum P_2^{IR} of −0.24 for infrared dichroism an angle of 69° between the C=O stretch direction and the main chain is found using eqs 10 and 11. Now the infrared dichroism data can be scaled on the WAXS and birefringence results.

In Figure 12 three depth profiles of the scaled order parameter are shown of films with different draw ratios. The orientation at the surface is of the same order of magnitude for every draw ratio. However, removing surface layers by careful grinding shows a draw ratio dependent decrease of the order parameter. The symmetry of the depth profile indicates that the measured decrease of orientation is not just an effect of the grinding. For the high draw ratios P_2 is less thickness dependent than at the lower draw ratios. This observation agrees with the results of Kaito et al.,[3,4] who found that the orientation function of extruded strands and sheets of a thermotropic copolyester increased with

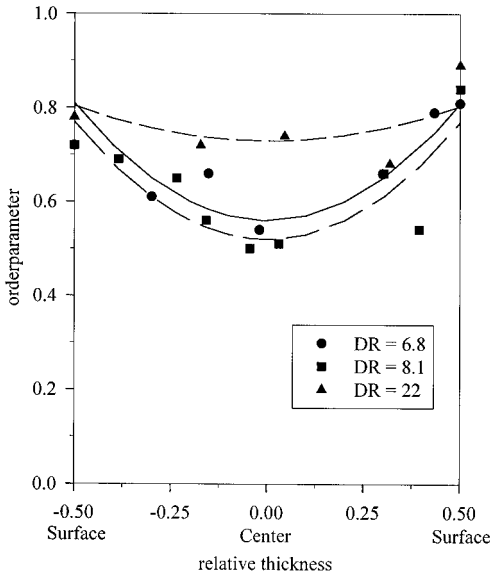

Figure 12. Depth profiles of the order parameter for three films with different draw ratios. The lines are drawn to guide the eye.

increasing draw ratio and with decreasing diameter of the die outlet. Figure 12 shows that the flow profile looks like a parabola. Averaging the order parameter over the thickness using either the parabola or a simple linear function does not differ much. Therefore, an average order parameter has been calculated by taking the mean of the values at the surface and at the center. These averages are shown in Figure 10. It is clear that the results of the infrared dichroism measurements correspond with the birefringence data better than the WAXS results, although there is still a considerable amount of scatter in the data (each point is a single measurement).

Discussion

The present results demonstrate the possibility of determining the birefringence of highly scattering solid films of thermotropic LCPs by means of the spectrographic method. Due to depolarization and polarization mixing effects, the amplitude of the measured oscillations is very small as compared to results obtained for lyotropic systems.[21,22] Nevertheless, meaningful values for Δn can easily be obtained by counting the numbers of zero crossings per unit wavelength. This spectrographic method can, therefore, be expected to be a new tool for investigations of the rheological behavior of thermotropic LCPs, providing the scattering of flowing systems is not very much larger than that of the solid films. Flow birefringence measurements showing the potential and limitations of this technique will be reported later.

The interpretation of the birefringence results of the drawn solid films in terms of an order parameter is not straightforward, as the comparison with the WAXS and infrared results shows. This is partly due to the lack of knowledge of the structure of the material and of the consequences of the preparation method and partly due to the different meanings of the results of different techniques.

The structure of drawn films of thermotropic LCPs is complicated. From polarized optical microscopy it is clearly visible that all our samples, even at the highest draw ratios, are built up of domains. No monodomain structures were seen. Scanning electron microscopy showed that the films are made up of discrete layers (thickness of the order of 1 μm) parallel to the film surface. A similar layered structure is proposed as an explanation for the residual normal stresses in the absence of shear stresses in the LCP Vectra A900.[29] The present infrared dichroism results indicate that different layers possess a different degree of orientation. Furthermore, differences in the degree of orientation may exist between the crystalline and quenched nematic parts of the material within the layers, differences which vary between the layers.

The distribution of orientations over the thickness of the samples is the result of the preparation process: extrusion and subsequent drawing and cooling. It is difficult to describe the deformation distribution over the sample thickness because the flow profile is not sufficiently known. Within the die, shear flow is predominant and most of the deformation will be near the wall because of the shear thinning behavior of the melt. Outside the die, extensional flow and solidification compete. At low draw ratios the material in the center of the film is not much extended after it has left the die; at high draw ratios it is.

The birefringence results represent an average over all textural entities throughout the thickness of the sample and, therefore, represent an average orientation of the entire sample. In comparing these results with WAXS results, which also entail a thickness averaging, one should keep in mind that this latter technique mainly samples the orientation of the crystalline parts (see below). Comparison of the birefringence measurements with measurements of dichroism by DRIFT is straightforward provided a complete thickness profile of the dichroism has been measured.

Figure 10 shows that the birefringence data follow the Kuhn and Grün equation for affine deformation quite well, although it could also be said that this equation is the lower bound of the experimental data. Adjusting the exponent of the draw ratio in the Kuhn and Grün equation from $-3/2$ to -2 yields the upper bound of the data. This suggests that the coefficient is somewhere between the two, indicating a slightly overaffine deformation process. Usually, the deformation process for flexible polymers in the molten state is described quite well by the affine function. It is not clear whether the small deviation from the affine behavior is caused by the liquid crystalline nature of the material or by the preparation method, i.e. drawing of films having an initial orientation due to the flow through the die. Of course, it would have been better to prepare oriented films by drawing isotropic films, because in that way the orientation introduced in the extruder would have been avoided. Unfortunately, drawing of compression molded (isotropic) samples was found impossible.

The thickness averaged infrared dichroism data show an affine behaviour as well (Figure 10), although less data are available. As stated in the results, we calculated the average order parameter by taking a linear decrease of orientation from the skin to the center of the film. Using a square relationship did not improve the agreement between the infrared dichroism data and the Kuhn and Grün curve.

From the data gathered in Figure 10 it can be concluded that the orientation of the crystalline part develops differently from the orientation of the entire sample as a function of the draw ratio. The orientation process of the crystalline part appears to be highly

overaffine, contrary to the remaining part of the material. This has also been reported for several other LCPs.[4,11,46−48] One explanation put forward in literature for this discrepancy between the WAXS data and the results from other techniques invokes the easy rotation of the already existing domains.[11,48] Another explanation takes into account the nonisotropic orientation distribution at the capillary exit.[46,47] However, these explanations would predict overaffine behavior for results of all measurement techniques considered because neither explanation distinguishes between crystalline and noncrystalline (in our case quenched nematic) parts of the material. A possible alternative explanation should take into account the process of crystallization, which is usually very much accelerated by orientation of the melt. If this is the case for thermotropic LCPs as well,[17,49] crystallites will preferentially be formed in the regions of the highest orientation of the elongating films. Hence, at low draw ratios the orientation of the crystallites is higher than the average orientation. When the draw ratio increases, the differences even out. Therefore, at high draw ratios the crystalline orientation may be assumed to reflect the average orientation, which justifies the scaling of the results of the birefringence and the infrared measurements to the maximum order parameter as obtained from WAXS measurements.

Conclusion

We have demonstrated in this article that the birefringence of highly scattering solid films of thermotropic LCPs can be determined by the spectrographic method. The amplitude of the intensity oscillations as a function of the wavelength, although small, is sufficiently large for quantitative determination of birefringence. The spectrographic birefringence technique is, therefore, expected to be suitable for rheo-optical studies of thermotropic LCPs.

The interpretation of the degree of orientation as determined from measurements of birefringence, infrared dichroism, and WAXS is different for each of these techniques and is dependent on the techniques themselves and on the nature and preparation of the samples. The average orientation in the solid drawn films, as determined from birefringence and infrared dichroism measurements, follows the Kuhn and Grün equation for pseudo-affine deformation. Infrared dichroism results show that the orientation varies through the thickness of the film. The orientation derived from WAXS measurements is distinctly overaffine, which may be the consequence of orientation-induced crystallization.

Acknowledgment. The authors would like to thank R. R. van Puijenbroek and E. A. Klop of Akzo-Nobel research laboratories in Arnhem, the Netherlands, for the provision of their laboratory facilities and their skills. In particular, we thank Dr. S. J. Picken and Dr. M. G. Northolt for their useful discussions and their helpful suggestions. Furthermore, we thank Prof. W. R. Burghardt for his comments and advice in setting up the spectrographic equipment. This project was funded by the Netherlands Organization of Scientific Research (NWO).

References and Notes

(1) Blundell, D. J.; Chivers, R. A.; Curson, A. D.; Love, J. C.; MacDonald, W. A. *Polymer* **1988**, *29*, 1459.
(2) Barres, O.; Friedrich, C.; Jasse, B.; Noël, C. *Makromol. Chem., Macromol. Symp.* **1991**, *52*, 161.
(3) Kaito, A.; Kyotani, M.; Nakayama, K. *Macromolecules* **1991**, *24*, 3244.
(4) Kaito, A.; Kyotani, M.; Nakayama, K. *J. Polym. Sci.: Part B,* Polym. *Phys.* **1993**, *31*, 1099.
(5) Bensaad, S.; Jasse, B.; Noël, C. *Polymer* **1993**, *34*, 1602.
(6) Heynderickx, I.; Paridaans, F. *Polymer* **1993**, *34*, 4068.
(7) Hsiung, C. M.; Cakmak, C. M. *Int. Polym. Proc.* **1993**, *8*, 255.
(8) Turek, D. E.; Simon, G. P. *Polymer* **1993**, *34*, 2750.
(9) Jansen, J. A. J.; Paridaans, F. N.; Heynderickx, I. E. J. *Polymer* **1994**, *35*, 2970.
(10) Dreher, S.; Zachmann, H. G.; Riekel, C.; Engstrøm, P. *Macromolecules* **1995**, *28*, 7071.
(11) Voyiatzis, G.; Petekidis, G.; Vlassopoulos, D.; Kamitsos, E. I.; Bruggeman, A. *Macromolecules* **1996**, *29*, 2244.
(12) Mercx, F. P. M. *Kunstst. Rubber* **1992**, *8*, 12.
(13) Graziano, D. J.; Mackley, M. R. *Mol. Cryst. Liq. Cryst.* **1984**, *106*, 73.
(14) Alderman, N. J.; Mackley, M. R. *Faraday Discuss. Chem. Soc.* **1985**, *79*, 149.
(15) Navard, P.; Zachariades, A. E. *J. Polym. Sci.: Part B, Polym. Phys.* **1987**, *25*, 1089.
(16) Hsiao, B. S.; Stein, R. S.; Deutscher, K.; Winter, H. H. *J. Polym. Sci.: Part B,* Polym. *Phys.* **1990**, *28*, 1571.
(17) Nicholson, T. M.; Mackley, M. R.; Windle, A. H. *Polymer* **1992**, *33*, 434.
(18) Srinivasarao, M.; Garay, R. O.; Winter, H. H.; Stein, R. S. *Mol. Cryst. Liq. Cryst.* **1992**, *223*, 29.
(19) De'Nève, T.; Navard, P.; Kléman, M. *J. Rheol.* **1993**, *37*, 515.
(20) Burghardt, W. R.; Fuller, G. G. *Macromolecules* **1991**, *24*, 2546.
(21) Hongladarom, K.; Burghardt, W. R.; Baek, S. G.; Cementwala, S.; Magda, J. J. *Macromolecules* **1993**, *26*, 772.
(22) Hongladarom, K.; Burghardt, W. R. *Macromolecules* **1993**, *26*, 785.
(23) Hongladarom, K.; Secakusuma, V.; Burghardt, W. R. *J. Rheol.* **1994**, *38*, 1505.
(24) Larson, R. G.; Mead, D. W. *Liq. Cryst.* **1992**, *12*, 751.
(25) Picken, S. J.; Aerts, J.; Doppert, H. L.; Reuvers, A. J.; Northolt, M. G. *Macromolecules* **1991**, *24*, 1366.
(26) Vermant, J.; Moldenaers, P.; Picken, S. J.; Mewis, J. *J. Non-Newtonian Fluid Mech.* **1994**, *53*, 1.
(27) Mortier, M. Rheology and texture of liquid crystalline polymers. Ph.D. thesis, Catholic University of Leuven, Belgium, 1995.
(28) Burghardt, W. R.; Bedford, B.; Hongladarom, K.; Mahoney, M. *ACS Symp. Ser.* **1995**, *597*, 308.
(29) Langelaan, H. C.; Gotsis, A. D. *J. Rheol.* **1996**, *40*, 107.
(30) Langelaan, H. C.; Posthuma de Boer, A. *Polymer*, in press.
(31) Saupe, A.; Maier, W. *Z. Naturforsch.* **1961**, *16A*, 816.
(32) Larson, R. G.; Doi, M. *J. Rheol.* **1991**, *35*, 539.
(33) Hall, M. M.; Veeraraghavan, V. G.; Rubin, H.; Winchell, P. G. *J. Appl. Crystallogr.* **1977**, *10*, 66.
(34) Sack, R. A. *J. Polym. Sci.* **1961**, *54*, 543.
(35) Northolt, M. G. Personal communication, 1994.
(36) Willems, C. R. J. A Dielectric study of melting and crystallization of semi-rigid and flexible-chain polymers. PhD thesis, Delft University of Technology, The Netherlands, 1995.
(37) Korte, E. H. *Vib. Spectrosc.* **1990**, *1*, 179.
(38) Jansen, J. A. J. *Hyphenated FT-IR techniques for the analysis of polymers.* PhD-thesis, University of Utrecht, The Netherlands, 1992.
(39) Fraser, R. D. B. In *A laboratory manual of analytical methods of protein chemistry*; Alexander, P., Block, R. J., Eds.; Pergamon Press: Oxford, U.K., 1960; Vol. 2, chapter 9, p 320.
(40) Kumar, S.; Stein, R. S. *J. Appl. Polym. Sci.* **1987**, *34*, 1693.
(41) Kuhn, W.; Grün, F. *Kolloid Z.* **1942**, *101*, 248.
(42) Ward, I. M. *Proc. Phys. Soc.* **1962**, *80*, 1176.
(43) Hamza, A. A.; Sikorski, J. *J. Microsc.* **1978**, *113*, 15.
(44) Wilson, D. J.; Vonk, C. G.; Windle, A. H. *Polymer* **1993**, *34*, 227.
(45) Voice, A. M.; Bower, D. I.; Ward, I. M. *Polymer* **1993**, *34*, 1154.
(46) Dibenedetto, A. T.; Nicolais, L.; Amendola, E.; Carfagna, C.; Nobile, M. R. *Polym. Eng. Sci.* **1989**, *29*, 153.
(47) Radler, M. J.; Landes, B. G.; Nolan, S. J.; Broomall, C. F.; Chritz, T. C.; Rudolf, P. R.; Mills, M. E.; Bubeck, R. A. *J. Polym. Sci.: Part B,* Polym. *Phys.* **1994**, *32*, 2567.
(48) Bruggeman, A.; Buijs, J. A. H. M. *Polymer*, in press.
(49) Langelaan, H. C. Rheological studies of thermotropic liquid crystalline polymers; PhD thesis, Delft University of Technology, The Netherlands, 1995.

MA960860T